J. Membrane Biol. 66, 123–132 (1982)

The Journal of
Membrane Biology

Microelectrode Studies of the Effect of Lanthanum on the Electrical Potential and Resistance of Outer and Inner Cell Membranes of Isolated Frog Skin

H. Goudeau*, J. Wietzerbin*, E. Mintz*, M.P. Gingold*, and W. Nagel**

* Service de Biophysique, Départment de Biologie, CEN Saclay 91191 Gif Sur Yvette Cedex, France and
** Physiologisches Institut der Universität München, Pettenkoferstrasse 12, D-8000 München 2, Germany

Summary. Microelectrodes were used to investigate the effect of 0.5 mM mucosal lanthanum (La^{3+}) on the intracellular potential and the resistance of outer and inner isolated frog skin (*Rana esculenta*) cell membranes. Under short-circuit conditions, the transapical membrane potential V_o^{sc} (mean value $= -65.4 \pm 3.2$ mV, inside negative) hyperpolarized to -108.7 ± 2.3 mV in control skins, after addition of the sodium blocker amiloride. Current-voltage curves for the outer and inner membranes were constructed from the amiloride-inhibitable current versus the outer membrane potential V_o or the inner membrane potential V_i. The outer, and to a lesser degree the inner, membrane showed a characteristic nonlinearity with two slope resistances. Addition of La^{3+} to the outer medium increased the short-circuit current to 190% of the control value. V_o^{sc} concomitantly changed to -28 ± 3.5 mV and outer and inner membrane resistances fell, considerably attenuating the nonlinearity seen in control skins. La^{3+} is suggested to raise the conductance by its effect on the surface potential. A secondary long-term inhibitory effect of La^{3+} on short-circuit current has been observed. It is ascribed to the penetration of La^{3+} into the sodium channels.

Key words frog skin · microelectrodes · *IV* curves · lanthanum

Introduction

According to the well-known model of Koefoed-Johnsen and Ussing (1958) for transepithelial active sodium transport, Na^+ traverses the epithelial cells by passive entry through the outer membrane and is then actively extruded through the inner or serosal membrane by a $(Na^+ + K^+)$-ATPase. This active sodium transport can be electrically described by a transepithelial driving force E_{Na} in series with a resistance R_{Na} representing the Na^+ active transport pathway (Ussing & Zerahn, 1951). When lanthanum (La^{3+}) is added to the outer side of the isolated frog skin, its initial effect is to increase the active epithelial Na^+ transport, measured as short-circuit current (Martinez-Palomo, Erlij & Bracho, 1971; De Sousa, 1975; Wietzerbin, Goudeau & Gary-Bobo, 1977; Grinstein, Candia & Erlij, 1978; Goudeau, Wietzerbin & Gary-Bobo, 1979). This transport stimulation is thought to arise from enhanced permeability of the outer membrane as a result of a surface effect of the trivalent ion which modifies the transapical membrane potential (Grinstein et al., 1978) and possibly intrinsic membrane conductance (Goudeau et al., 1979). However, at present, only a rise in the overall conductance of the active pathway $\left(g_{Na} = \frac{1}{R_{Na}}\right)$ has been evidenced, without any significant change in E_{Na} (Goudeau et al., 1979). On the other hand, La^{3+} stimulation of Na^+ transport is transient, since La^{3+} presumably has a secondary longterm inhibitory effect on the Na^+ permeability of the outer membrane.

The present study uses a recently developed microelectrode technique to measure intracellular potentials in frog skin epithelium (Nagel, 1976, 1977, 1978, 1980; Helman & Fischer, 1977). On control and La^{3+}-treated skins, we measured the outer membrane potential V_o at different transepithelial potentials (V_{CL}), with and without the specific sodium transport blocker amiloride. We established a nonlinear relationship between amiloride-inhibitable current (i.e. Na^+-active current), and the transmembrane potentials.

We observed that La^{3+}:

1) changes the outer cell membrane electrical gradient existing under short-circuit conditions;

2) increases outer membrane conductance and to a lesser degree inner membrane conductance;

3) flattens the rectification exhibited by both membranes, and

4) has a long-term effect mainly manifested by a secondary decrease in outer membrane conductance.

0022-2631/82/0066-0123 $02.00

Materials and Methods

List of Symbols

V_{CL}	transepithelial clamping voltage (inside positive)
V_o, V_i	potential differences across the outer and inner membranes ($V_o = V$ cell $- V$ outer medium; $V_i = V$ inner medium $- V$ cell; $V_{CL} = V_o + V_i$)
V_o^{sc}	intracellular potential under short-circuit conditions
V_{oamil}^{sc}	V_o^{sc} but with amiloride in the outer Ringer's medium
I	transepithelial current (positive from outer to inner side)
I_{Na}	amiloride inhibitable current
I^{sc}	short-circuit current
E'_1, $E'_{1\,amil}$	transepithelial clamping potential when $V_o = 0$ mV without and with amiloride
E_{Na}	electromotive force for active transepithelial Na^+ transport ($E_{Na} = I_{Na} \cdot R_{Na}$)
E_o, E_i	equilibrium potentials of the outer and inner membranes
R_{Na}, g_{Na}	resistance and conductance of the active sodium pathway
R_o, g_o, R_i, g_i	resistance and conductance of the active sodium pathway for the outer and inner membranes
$F(R_o)$	fractional resistance of the outer membrane: ($F(R_o) = R_o/(R_o + R_i)$ calculated from $\Delta V_o/\Delta V_{CL}$).

Methods

The microelectrode technique used was essentially the same as described by Nagel (1976, 1977, 1978, 1980) and Helman and Fisher (1977). Isolated abdominal skins of *Rana esculenta* were mounted horizontally with the outer side upwards. The skin, supported by a copper grid on the serosal side, was maintained in a special Ussing-type chamber with an open outer side for the impalements. The outer and inner compartments (0.4 ml each) where continuously perfused with normal Ringer's at a rate of 10–15 ml and 3–5 ml/min, respectively. The microelectrodes were prepared from 1.5 mm outer diameter microfiber capillaries (Clark electro-medical instruments) and back-filled with 1.5 M KCl. They were only used with input resistances and tip potentials of 15 to 40 MΩ and of less than 5 mV. The measurements were considered valid when the tip potential of the microelectrode, measured in the Ringer's solution, did not change by more than 3 mV before and after impalements. Skins were continuously short-circuited by an automatic clamping device, except during the current-voltage curve determinations. For this purpose, skins were clamped at V_{CL} (−60 to 160 mV, with outer side grounded) in steps of 10 mV. The transepithelial potential V_{CL} was maintained for 500 msec, which sufficed to bring I and V_o to steady state (Nagel, 1977; Helman, 1979). The current-voltage curves, established with and without amiloride were used to determine transepithelial conductance, fractional resistance of the apical membrane and conductance of the outer and inner membranes. Digital print-outs of the intracellular and transepithelial data were entered on a desk-calculator (Hewlett-Packard, type 9825) and used for the calculations. They were plotted automatically by a calculator-commanded plotter. In addition, I and V_o were continuously registered on a two-channel pen-recorder (Sefram, Paris).

Solutions

Normal Ringer's was used throughout the experiments and contained (in mM): 110 NaCl, 2.5 KCl, 1 $CaCl_2$, 1 $MgCl_2$ and 5 Tris-HCl (pH 7.5). La^{3+} as acetate or nitrate salt was added to the outer Ringer's up to a final concentration of 0.5 mM. Amiloride (a gift from Merck, Sharp and Dohme, France) was used at concentrations from 5×10^{-8} to 1×10^{-4} in the outer Ringer's: small doses of amiloride were repetitively added until the I^{sc} became minimal and unsensitive to further addition of the blocker. All the given data have been calculated for 1 cm^2 skin area.

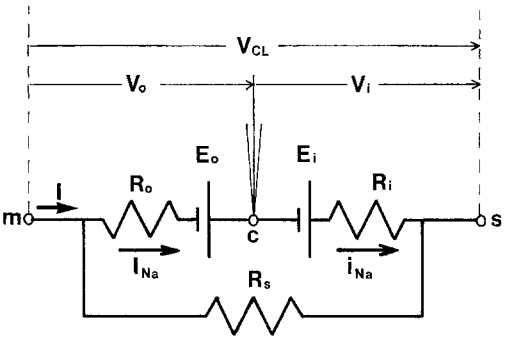

Fig. 1. Equivalent circuit-model of the skin. *m*, *c*, and *s* are mucosal, cellular, and serosal compartments, respectively. R_s is the shunt resistance. All other symbols are defined in the text

Sequence of Measurements

Impalement criteria are those defined by Nagel (1976, 1978). Once the cell was impaled and reliable V_o^{sc} values were obtained, amiloride was added to block sodium transport: when I_{amil}^{sc} and V_{oamil}^{sc} had attained stable values (less than 2 min), measurement of the $I-V$ relationship was made. Amiloride was then removed, V_o^{sc} and I^{sc} were allowed to return to their initial values (4–5 min) and another $I-V$ determination was made as before. We verified for *Rana esculenta* under control conditions that the steady state is reached within 500-msec duration of the voltage clamp (characteristically between 100 to 200 msec). This sequence of measurements is referred to as control measurements.

On their completion La^{3+} was added and when maximal stimulation was reached (3–10 min) $I-V$ determinations were made as before and after addition of amiloride to the La^{3+} Ringer's (experimental measurements). In five experiments, the long-term effects of La^{3+} were followed on the same impaled cell for over 1 hr.

Determination of Electrical Parameters

We used the simple electrical model shown in Fig. 1 (Schultz, Frizzell & Nellans, 1977; Nagel, 1978; Helman, 1979, Schultz, 1979). Under steady-state transporting conditions, V_o, V_i and V_{CL} are expressed as:

$$V_o = E_o - I_{Na} R_o \tag{1}$$

$$V_i = E_i - I_{Na} R_i \tag{2}$$

$$V_{CL} = E_o + E_i - I_{Na}(R_o + R_i). \tag{3}$$

From Eqs. (1) and (3) we deduce that:

$$V_o = \frac{E_o R_i + V_{CL} R_o - E_i R_o}{R_o + R_i}. \tag{4}$$

Under short-circuit conditions,

$$V_{CL} = 0 \quad \text{and} \quad V_o = -V_i = V_o^{sc}$$

where

$$V_o^{sc} = \frac{E_o R_i - E_i R_o}{R_o + R_i}. \tag{5}$$

If amiloride only increases outer membrane resistance ($R_o \gg R_i$), without affecting the outer electrical parameters, then it readily appears from Eq. (5) that $V^{sc}_{o\,amil} = -E_i$. From Eqs. (4) and (5) we can write:

$$V_o = V_{CL}\frac{R_o}{R_o+R_i} + V^{sc}_o. \tag{6}$$

For $V_o = 0$ mV the clamp potential is written as E'_1 (Helman & Fisher, 1977):

$$E'_1 = -\frac{R_o+R_i}{R_o}\cdot V^{sc}_o. \tag{7}$$

Relations (5) and (7) yield:

$$E'_1 = E_i - E_o\frac{R_i}{R_o}. \tag{8}$$

Thus E'_1 is only equal to E_i (Helman, 1979) when $E_o \simeq 0$ and/or $R_o \gg R_i$. With amiloride ($R_o \gg R_i$) from Eqs. (7) and (8), $E'_{1\,amil} = -V^{sc}_{o\,amil} = E_i$.

Amiloride is thought to block selectively the entire sodium transcellular current (Crabbé, 1968; Dörge & Nagel, 1970). In fact under our experimental conditions, the value of the residual current after amiloride (I_{amil}) is 2.25 ± 0.25 μA/cm², i.e. 7.5 ± 0.8 % of the total current (3.4 ± 0.3 % after La^{3+}). The transcellular current I_{Na} was obtained by calculating $I_{Na} = I - I_{amil}$ (Fig. 1) for each value of V_{CL} (Fuchs, Hviid Larsen & Lindemann, 1977; Schultz, 1979). It is then possible to plot I_{Na} versus V_o. Assuming that amiloride had no effect on electrical parameters, except R_o, within 1–2 min after application, we graphically deduced E_o and R_o from Eq. (1). As $V_i = V_{CL} - V_o$, we also plotted $I_{Na} = f(V_i)$ and obtained, from Eq. (2), E_i and R_i. As pointed out by Nagel (1980), R_i can be estimated directly from the difference in V^{sc}_o and I^{sc} before and after amiloride [relation (2)]. Remembering that in short-circuit conditions $V^{sc}_o = -V^{sc}_i$, this yields:

$$R_i = \frac{V^{sc}_o - V^{sc}_{o\,amil}}{I^{sc} - I^{sc}_{amil}} = \frac{\Delta V^{sc}_o}{I^{sc}_{Na}}.$$

For $I_{Na} = 0$, the plot of $I_{Na} = f(V_{CL})$ gives the operational value of the Na^+ active electromotive force E_{Na} [$E_{Na} = E_o + E_i$, relation (3)].

Results

Short-Term Effects of La^{3+}

Figure 2 (*a*, *b*) shows the typical evolution of I and V_o before (*a*) and after (*b*) 0.5 mM addition of La^{3+}. I^{sc} increased within about 2 min of La^{3+} addition from 22 to 49 μA. This increase (123 % of the control value) was accompanied by a depolarization of the cell from −76 to −32.5 mV (mean values of these parameters are given in Table 1). Amiloride has similar effects on control and La^{3+}-treated skins.

Figure 3*a* (control) and 3*b* (La^{3+}) are constructed with the data shown in Figs. 2*a* and 2*b*. On control skin (Fig. 3*a*), the $V_o - V_{CL}$ is nonlinear. Calculation of the individual values of $F(R_o)$ shows that $F(R_o)$ values increase slightly but continuously for V_{CL} values ranging from −30 to 30 mV (i.e. from 0.57 to 0.61 in Fig. 3*a*), steeply for V_{CL} ranging from 40 to 70 mV and again slowly beyond $V_{CL} = 80$ mV (i.e. 0.77 and 0.82 for V_{CL} equal, respectively, to 80 and 120 mV). Consequently, two mean $F(R_o)$ values can be approximated by two slopes in the $V_o = V_{CL}$ curve. The first (labeled $1 = F(R_0)_1$) corresponds to the region of depolarized outer membrane (i.e. for V_{CL} higher than 80 mV), and the second (labeled $2 = F(R_o)_2$) to small excursions of V_o around V^{sc}_o. Mean values of $F(R_o)_1$ and $F(R_o)_2$ obtained on 13 experiments are, respectively, 0.802 ± 0.025 and 0.526 ± 0.033. As indicated in Table 1, $F(R_o)_1$ and $F(R_o)_2$ are significantly different in control values. Accordingly, the resistance of the epithelial cell barriers is not constant when the transmembrane electrical gradient alters. The effect of amiloride is to linearize the curve perfectly (mean $F(R_o)_{amil} = 0.965 \pm 0.008$). As theoretically expected, $V^{sc}_{o\,amil}$ and $E'_{1\,amil}$ values are not different.

On La^{3+}-treated skins (Fig. 3*b*), two $F(R_o)$ can also be defined (Table 1) and as in control skins, amiloride linearizes perfectly the $V_o - V_{CL}$ curve. In contrast to $V^{sc}_{o\,amil}$ and $E'_{1\,amil}$ values which do not alter compared to the control, E'_1 is significantly decreased by La^{3+} (66.4 ± 6.4 mV *vs.* 95.5 ± 3.6 mV).

Mean values for V^{sc}_o, $V^{sc}_{o\,amil}$, E'_1, $E'_{1\,amil}$, $F(R_o)$ and $F(R_o)_{amil}$ are given in Table 1 for control and experimental measurements.

Figures 4*a* and 4*b*, also constructed with the data obtained from the experiment depicted in Figs. 2*a* and 2*b*, show the evolution of I, I_{amil} and I_{Na} versus V_{CL}. In control skin, the $I - V_{CL}$ curve is obviously not linear. This nonlinearity is more pronounced for the $I_{Na} - V_{CL}$ curve. Two slope resistances $R_{Na\,1}$ and $R_{Na\,2}$ (8,600 ± 2,000 and 3,840 ± 640 Ω cm²) are operationally defined at the intercepts of the curve with V_{CL} axis and I axis (these points are labeled, respectively, 1 and 2 on the figures). The value of V_{CL} which yields $I_{Na} = 0$ corresponds to the E_{Na} value for sodium active transport. The mean value obtained (119 ± 6 mV) is in the range of the values obtained on frog skins with other methods (Helman & Fisher, 1977). As seen in Fig. 4*a* and 4*b*, the $I_{amil} - V_{CL}$ curves are linear from 0 to 120–140 mV in all the skins studied but some skins displayed a second slope resistance for negative V_{CL} values.

On La^{3+}-treated skins (Fig. 4*b*), the I^{sc} increases (Table 1). As previously reported (Wietzerbin et al., 1977), the resistance of the Na^+ active pathway decreases concomitantly with the increase in I^{sc}. This decline is more evident for $R_{Na\,1}$ than $R_{Na\,2}$ (Table 1), and consequently the ratio $R_{Na\,1}/R_{Na\,2}$ diminished for La^{3+}-treated skins from 2.24 to 1.32 compared to control skins. The value of E_{Na} in La^{3+}-treated skins is not different from the control skin value (122 ± 6.5 *vs.* 119 ± 6 mV).

The nonlinearity seen on curves 4*a* and 4*b* may be due to either epithelial barrier or both. Figure 5*a*

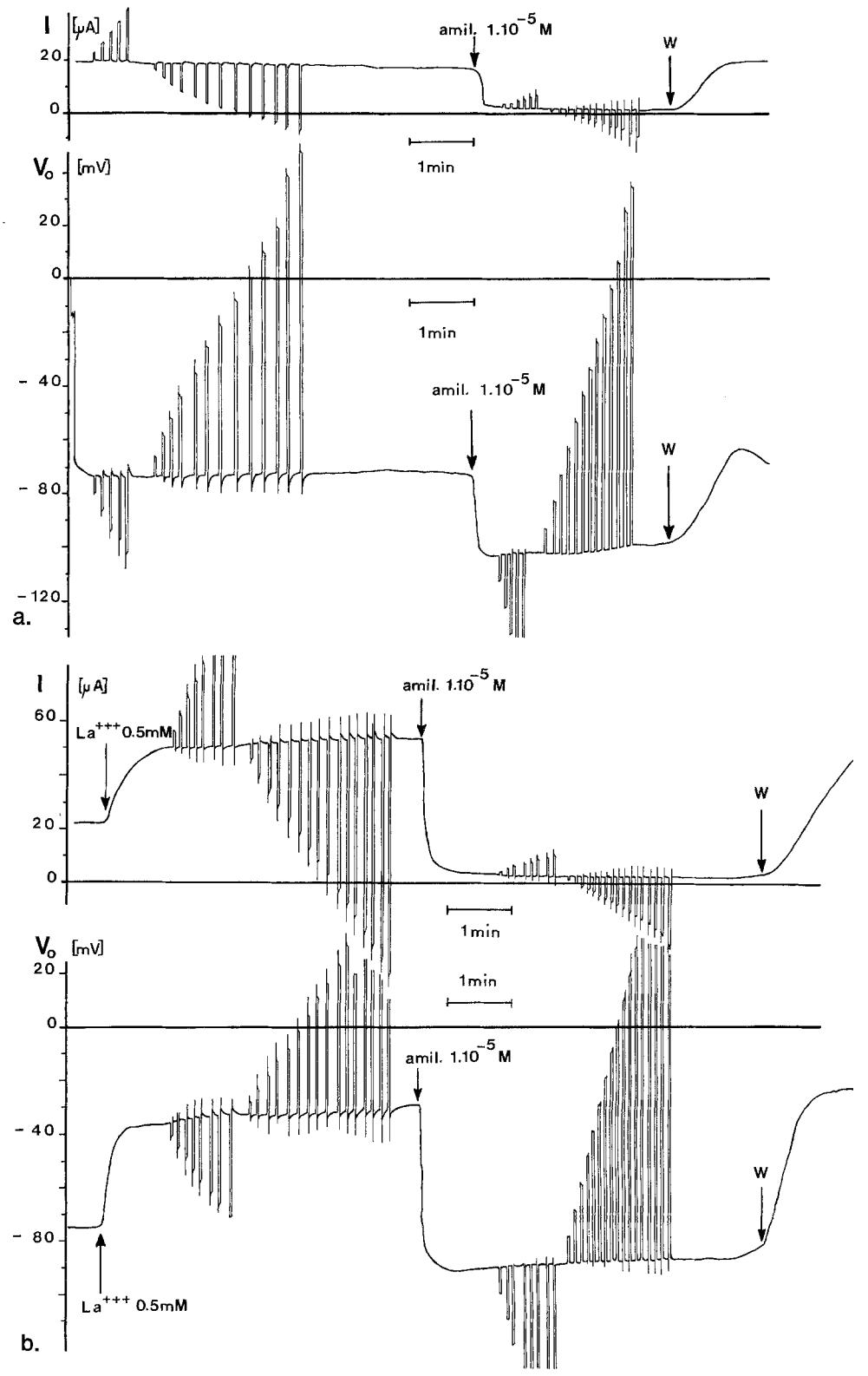

Fig. 2. (*A*) Evolution of the current I and the transapical potential V_o. Upper curve shows the evolution of the current during the control period. The permanently short-circuited skin (I^{sc} conditions), is clamped for 500 msec from 0 to -40 mV (serosal side negative) and from 0 to 130 mV (serosal side positive) in steps of 10 mV. The resulting variation in current is registered. Amiloride (1×10^{-5} M) is then added on the mucosal side (perfusion rate 10 ml/min), and the same measurements are made. The arrow indicates the washout of amiloride; the lower curve shows the evolution of the transapical potential V_o (cell negative). Upon microelectrode penetration into the cell, a stable potential (V_o^{sc}) is attained in less than 1 min. The V_o value is registered for each clamp voltage; amiloride causes instantaneous hyperpolarization of V_o^{sc}. (*B*) *Upper curve*: at the arrow, La^{3+} is added on the mucosal side at a final concentration of 0.5 mM. The short-circuit current increases and reaches a maximum in approximately 2 min. The same measurements were made as for the control period. *Lower curve*: as the I^{sc} increases, the apical membrane depolarizes. The currents shown have been registered through a 0.8-cm^2 skin area

Table 1.

		Control	La^{3+a}
I^{sc} ($\mu A/cm^2$)		29.6 ±5	57.9 ±8.1
R_{Na} ($\Omega\,cm^2$)	R_{Na1}	8,600±2,000	3,120±640
	R_{Na2}	3,840±640	2,360±440
R_o ($\Omega\,cm^2$)	R_{o1}	7,120±1,520	2,000±560
	R_{o2}	2,160±480	1,120±310
R_i ($\Omega\,cm^2$)	R_{i1}	1,200±200	1,280±170
	R_{i2}	1,760±344	1,360±160
R_i ($\Omega\,cm^2$) $=\Delta V_o^{sc}/I_{Na}^{sc}$		1,680±300	1,640±200
$F(R_o)$	$F(R_o)_1$	0.802±0.025[c]	0.53 ±0.04[c]
	$F(R_o)_2$	0.526±0.033[c]	0.374±0.02[c]
$F(R_o)_{amil}$		0.965±0.008	0.974±0.008
E_{Na} (mV)	$=(V_{CL})_{I_{Na}=0}$	119 ±6	122 ±6.5
	$=E_o+E_i$	122.5±6.5	125.5±6.5
E_o (mV) $=(V_o)_{I_{Na}=0}$		23.1±5.8	30.7±4.9
E_i (mV) $=(V_i)_{I_{Na}=0}$		100.8±2.5	92.6±4.4
V_o^{sc} (mV)		−65.4±3.2[c]	−28 ±3.5[c]
$V_{o\,amil}^{sc}$ (mV)		−108.7±2.3	−109.3±2.8
E_1' (mV)		95.5±3.6[b]	66.4±6.4[b]
$E_{1\,amil}'$ (mV)		109.7±3.5	111.9±3.9

[a] La^{3+} concentration: 0.5 mM.
[b] Values significantly different at $0.01<p<0.05$.
[c] Values significantly different at $p=0.01$. ($n=13$)

shows that in the present case the $I-V$ relationship displayed by the outer barrier is also strongly non-linear. Two slope resistances R_{o1} and R_{o2}, defined, respectively, at $I_{Na}=0$ and $I_{Na}=I_{Na}^{sc}$ (i.e. similar to the above operational definition of R_{Na1} and R_{Na2} and labeled in the same way), were deduced from the $V_o=f(I_{Na})$ curve with mean values of 7,120 ±1,520 and 2,160±480 $\Omega\,cm^2$, respectively (ratio 3.30). When $I_{Na}=0$, the V_o value gives E_o, the apparent electromotive force of the outer barrier. This value ($E_o=23.1\pm5.8$ mV) is significantly different from zero (at $p<0.01$). At the inner membrane level, two slopes R_{i1} and R_{i2} also appear (respectively, 1,200±200 and 1,760±344 $\Omega\,cm^2$, also defined at $I_{Na}=0$ and $I_{Na}=I_{Na}^{sc}$ and labeled 1 and 2). As the graphic determination of the slope R_{i1} is not very precise, the value of the ratio R_{i1}/R_{i2} must be considered with less confidence than the ratio R_{o1}/R_{o2}. However, Fig. 5*a* shows that the change in R_i slope is steeper than in the case of R_o. Estimation of R_i calculated as $\Delta V_o^{sc}/I_{Na}^{sc}$ gives a value of $R_i=1{,}680$ ±300 $\Omega\,cm^2$, which is practically identical to the R_{i2} value.

The effects of La^{3+} are seen in Fig. 5*b*. La^{3+} reduces R_{o1} and R_{o2}, respectively ($R_{o1}/R_{o2}=1.80$), to 28 and 52% of their control values. As already noted for R_{Na} the effect of La^{3+} is clearly more pronounced on R_{o1} than on R_{o2} region. This decrease in R_{o1}

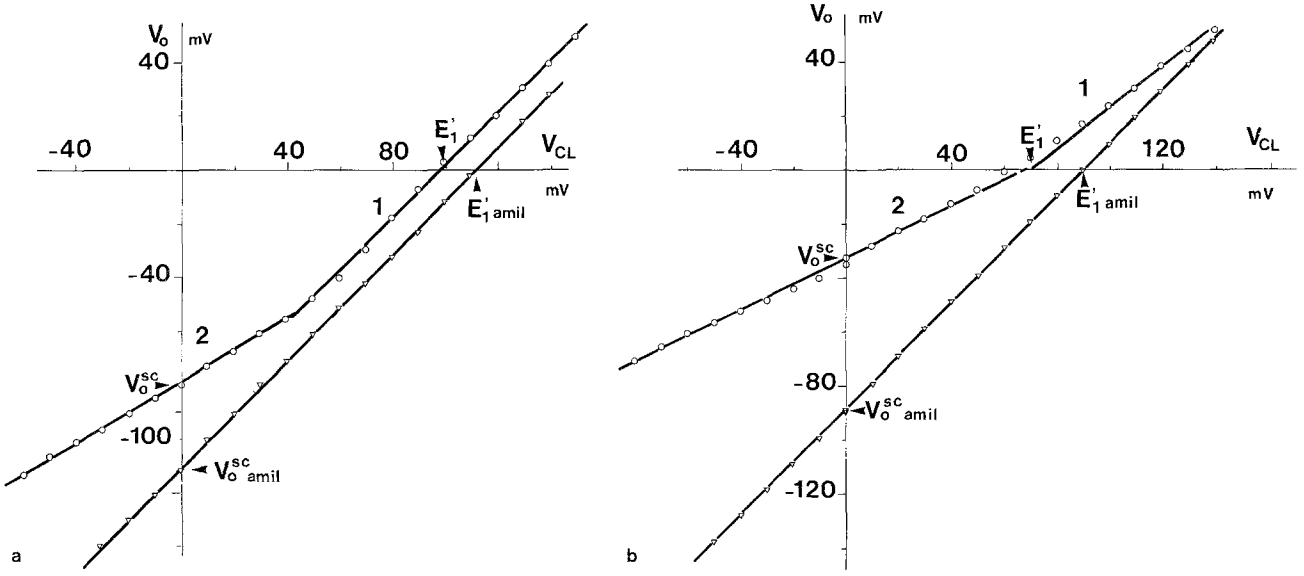

Fig. 3. Curve $V_o=f(V_{CL})$ without (*o*) and with (*Δ*) amiloride. (*A*) Control experiment: The Figure is constructed from the data in Fig. 2*a*. Two mean values of $F(R_o)$ (calculated as $\Delta V_o/\Delta V_{CL}$) are obtained: $F(R_o)_1=0.92$ when the apical membrane is depolarized (portion 1 of the curve) and $F(R_o)_2=0.60$ when V_o is the range of the V_o^{sc} values (portion 2 of the curve). E_1' corresponds to the value of the clamp potential for which $V_o=0$ mV. With amiloride (*Δ*) the relation between V_o and V_{CL} is linear ($F(R_o)_{amil}=1$). (*B*) La^{3+} experiment: the Figure is constructed from the data in Fig. 2*b*. La^{3+} depolarizes the cell ($V_o^{sc}=-33$ mV *vs.* −78 mV on control) and diminishes the values of E_1' and $F(R_o)$ ($F(R_o)_1=0.76$ and $F(R_o)_2=0.48$). With amiloride $F(R_o)_{amil}$ is equal to 0.99

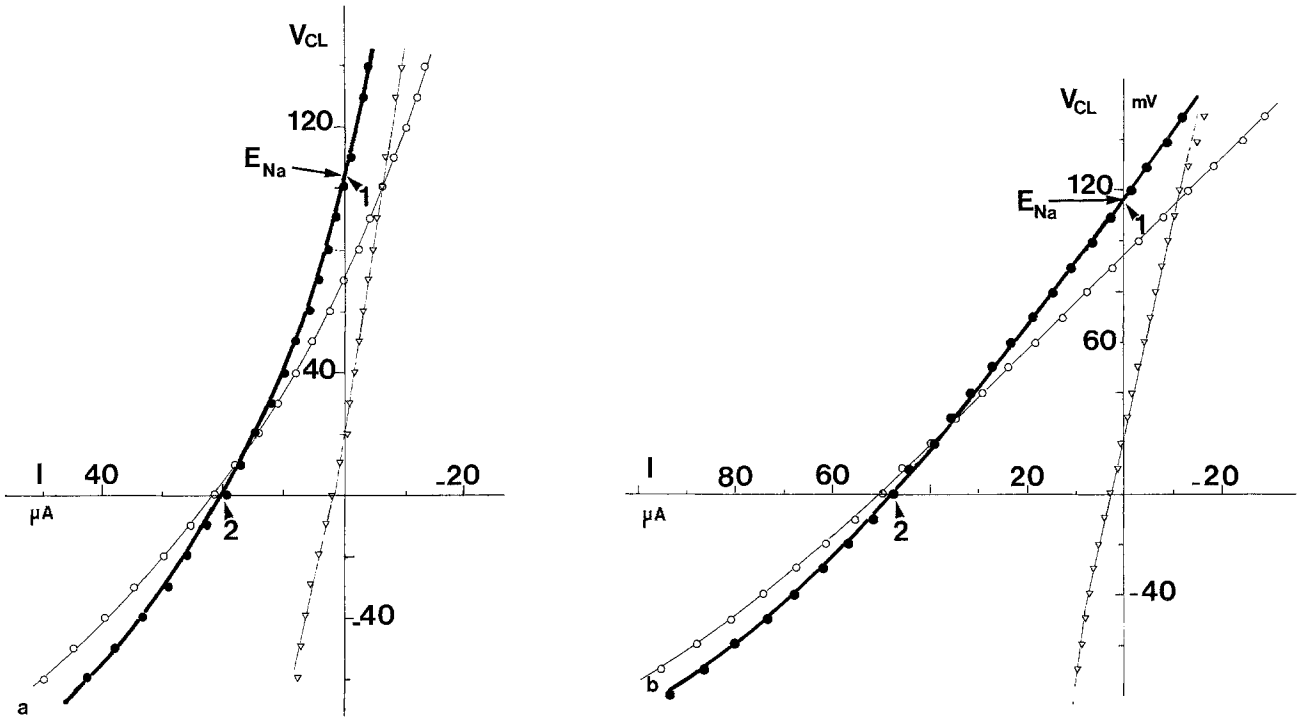

Fig. 4. Curves $I=f(V_{CL})$, $I_{amil}=f(V_{CL})$ and $I_{Na}=f(V_{CL})$. (*A*) Control experiment: the Figure is constructed from the data in Fig. 2*a*. The open symbols represent the evolution of transepithelial current as a function of the clamp potential V_{CL} without (*o*) and with (*Δ*) amiloride. The filled symbols (●) represent the amiloride-inhibitable current I_{Na} as a function of the clamp potential V_{CL}. The curve is constructed by subtracting the amiloride current from the total current at each clamp potential. At the intercepts of the curve with the *Y*-axis (point 1) and with the *X*-axis (point 2) two slope resistances can be measured. They correspond, respectively, to R_{Na1} and R_{Na2}. (*B*) La^{3+} experiment: the Figure is constructed from the data in Fig. 2*b*, and the same method as in the control experiment is used. The $I_{Na}=f(V_{CL})$ is nearly linear and R_{Na1} and R_{Na2} have practically the same values

is accompanied by an augmentation in E_o (30.7 ±4.9 mV). La^{3+} only alters R_{i1} and R_{i2} slightly since $R_{i1}=107\%$ of the control and $R_{i2}=77\%$ of the control. R_i calculated as $\Delta V_o^{sc}/I_{Na}^{sc}$ is not modified (97% of control). E_i calculated when $I_{Na}=0$ is smaller than the corresponding control value (*see* Table 2), and both values of E_i are different from their corresponding $V_{o\,amil}^{sc}$ values.

Long-Term Effects of La^{3+}

We previously reported (Goudeau et al., 1979) that the transient character of La^{3+} stimulation could be due to progressive blockage of the outer membrane sodium channels by the trivalent ion. In the present work we measured the evolution of the electrical parameters after 1 hr of La^{3+} action on five skins. Table 2 gives the values of these parameters at maximum stimulation and 1 hr later. The results in Table 2 are well-correlated with earlier findings concerning the long-term effects fo La^{3+} (Wietzerbin et al., 1977).

Discussion

The purpose of this study of the effects of La^{3+} on the electrical and electrochemical parameters underlying sodium transport across frog skin was to improve understanding of the mechanism by which Na^+ permeates across the outer barrier of the epithelial cells. Our results can be summarized in three points:

1) The *Rana esculenta* skin was shown to exhibit nonlinearity in the $I_{Na}-V_{CL}$ curve which arises predominantly in the outer membrane.

2) Stimulation of Na^+ transport by La^{3+} was observed to be due to an interaction of the trivalent ion with the outer membrane. This stimulation reduced the resistance and linearizes I_{Na} current-voltage curve of the outer membrane, indicating that La^{3+} interferences with the molecular mechanism controlling the conductance process of the sodium channel.

3) We confirmed the secondary inhibitory effect of La^{3+} is located in the outer membrane.

Baseline Electrophysiological Data and Current-Voltage Relationships

Baseline Data. As reported by Nagel (1976, 1977, 1978, 1980) and Helman and Fisher (1977), V_o^{sc} was largely negative in the control skins (Table 1). Ami-

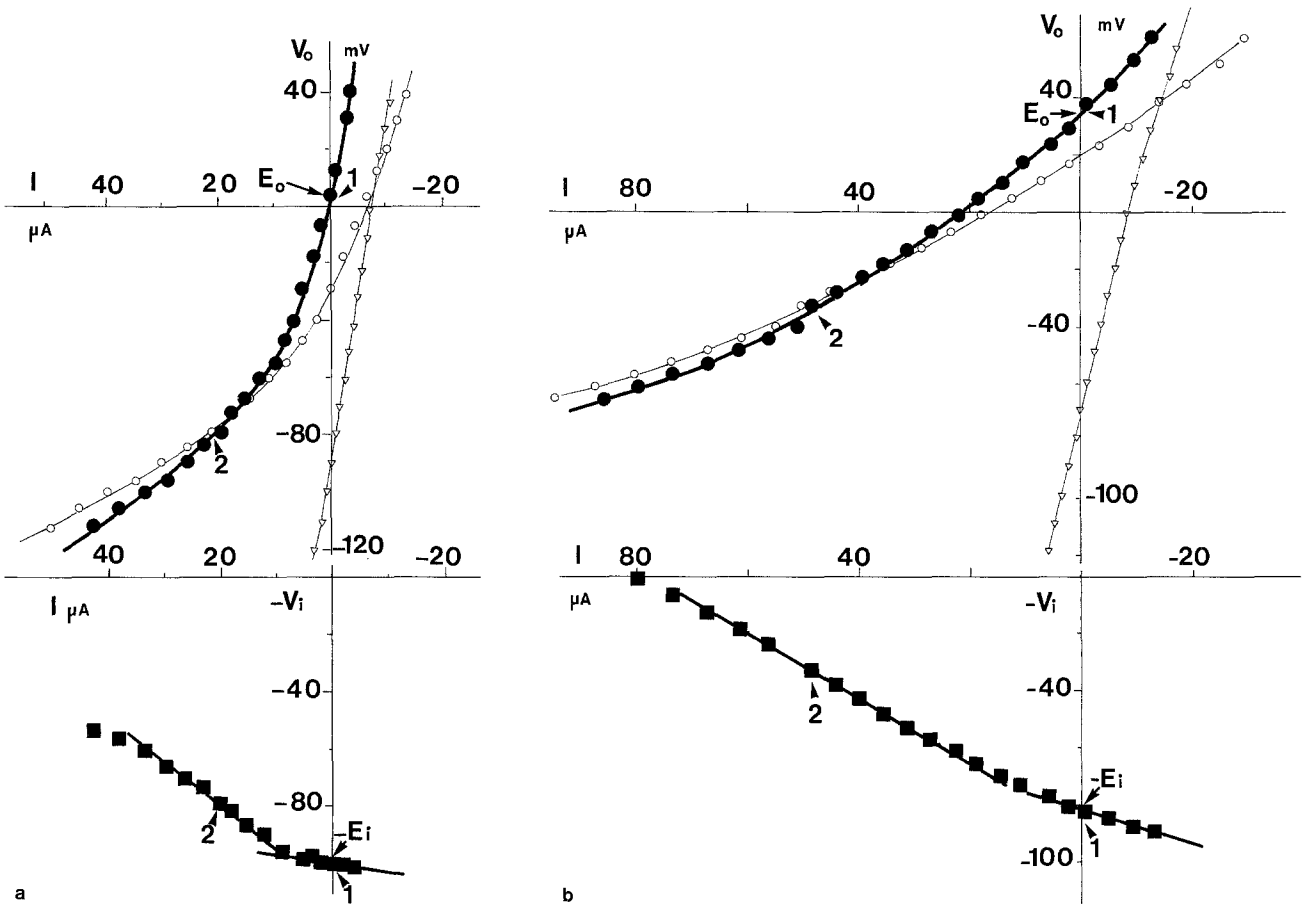

Fig. 5. Curves $V_o=f(I)$, $V_o=f(I_{amil})$, $V_o=f(I_{Na})$ and $-V_i=f(I_{Na})$. (*A*) Control experiment: this Figure is also constructed from the data in Fig. 2*a*. The open symbols represent the evolution of V_o as function of the transepithelial current without (*o*) and with (*Δ*) amiloride. The filled symbols represent the evolution of the transmembrane potentials as a function of the amiloride inhibitable current (I_{Na}). At each clamp potential V_{CL}, V_o has been measured and $-V_i$ and I_{Na} calculated to obtain the $V_o=f(I_{Na})$ curve (●) and the $-V_i=f(I_{Na})$ curve (■). The slope resistances R_{o1}, R_{o2}, R_{i1}, R_{i2} were defined at the points labeled 1 and 2 on their respective curves. (*B*) La^{3+} experiment: this Figure is constructed from data in Fig. 2*b*, and the same method used as in the experiment. Note that the nonlinearity of the curves relating V_o and V_i to I_{Na} is less pronounced than in the control situation

Table 2.

		I_{sc}	R_{o1}	R_{o2}	R_{i1}	R_{i2}	E_{Na}
Values as percent of control:	at max. stimulation (5–10 min after La^{3+} addition	194±19	27±4	46±5	107±10	77± 8	102±5
	1 h after La^{3+} addition	137±18	50±8	103±5	100±10	95±12	92±5

($n=5$) La^{3+} concentration: 0.5 mM.

loride raised V_o^{sc} (Fig. 2) as was expected from the blockage of the Na^+ current crossing the apical membrane.

Values of E_1' (95.5±3.6 mV) are smaller than those reported by Helman and Fisher (1977) and Nagel (1978) (125 and 108 mV, respectively). Taking into account the electrical model used [Eq. (8)], this difference appears to result mainly from the existence of an electromotive force E_o which is significantly different from zero at $p<0.01$ according to the Student *t*-test. ($E_o=23.1\pm5.8$ mV; Range of values: −8 to +55 mV: one value is negative, another null and the eleven positive).[1] This result is at variance with those of Helman and Fisher (1977) and Nagel (1978). In contrast to Nagel (1978) and Helman and Fisher (1977) who reported fractional re-

[1] In another experimental series, E_o was determined in the same condition as in control skins. The mean value obtained for E_o was 36.5±4.9 mV (Range: 27–62 mV, $n=8$). In this series, the mean I_{sc} and R_{o1}, R_{o2} values were, respectively, 39.5±3.5 μA/cm², 4,450±600 Ω and 1,440±170 Ω/cm². Thus E_o and I^{sc} values are higher and R_o smaller than in the present study.

sistance $F(R_o)$ in the range of 0.8, the value we measured was lower 0.653 ± 0.053). The reason is that in our study the values of R_i (Table 1) are distinctly higher than that reported by Nagel (1978) and Helman and Fisher (1977) on *Rana temporaria* and *Rana pipiens* (700–1,000 $\Omega\,cm^2$) at almost comparable R_o values ($2{,}160 \pm 480$ for our R_{o2} value *vs.* $2{,}600 \pm 300\ \Omega\,cm^2$). Species differences could account for this divergence. Possible leaks around the microelectrode at the impalement site to account for diminished values of R_o can be ruled out from the fact that $F(R_o)$ is practically equal to 1 (0.96) after amiloride.

Outer Membrane Current-Voltage Curve. The Ussing and Zerahn (1951) model implicitly postulates that frog skin behaves like a linear resistor. This assumption has very often been accepted (Biber & Sanders, 1973; Schultz et al., 1977; Schultz, 1979; Macknight, Di Bona & Leaf, 1980). However, nonedge-damaged frog skins have been reported to exhibit nonlinear $I-V$ curves which show a break point at transepithelial clamp voltages between some $+80$ and 130 mV (Helman & Miller, 1971; Helman & Fisher, 1977; Nagel, 1978; Macchia & Helman 1979). As the shunt pathway resistance was shown to be constant in these experiments, the origin of nonlinearity was obviously in the active Na^+ pathway (or at least the cellular pathway). Nonlinearity and constancy of the shunt pathway resistance are also obtained in the present investigation (*see* Figs. 4 and 5). Figure 5*a* and 5*b* indicate furthermore that nonlinearity of the $I-V$ relationships of the outer membrane is essentially responsible for this behavior. Such observation is at variance with the results of Helman and Fisher (1977) and with Helman's theoretical prediction (1979), reporting a constant Thevenin conductance of the apical membrane in the range of negative potential at the apical border and a change in the conductance upon reversal of the transapical potential gradient. Our data, in contrast, suggest continuous increase of the apical border resistance when the apical border is depolarized and the apical potential gradient reversed. At present it is difficult to provide a reasonable explanation of these differences. Nonlinearity of the $I_{Na}-V_o$ curve would be expected if sodium penetrates across the apical membrane by electrodiffusion (Biber & Sanders, 1973; Cuthbert & Shum, 1976; Fuchs et al., 1977), for a situation in which the Na^+ concentration of the outer solution is higher than inside the cell. Nevertheless, the Goldman constant field equation (Goldman, 1943) does not fit the $I_{Na}-V_o$ curves: by using the Goldman equation for different points of the curve it appears that the apparent permeability of the outer membrane decreases when V_o is varied from hyperpolarized values to zero. From the slope of I_{Na} *vs.* V_o in Fig. 5*a*, it can be derived that the resistance (dV_o/dI_{Na}) increases more than fourfold if V_o is changed from -80 to 0 mV. This exceeds by far what can be calculated from the constant field equation for change in integral resistance R_{Na} (Finkelstein & Mauro, 1963) at constant P_{Na} (1,55). Deviation from the behavior expected from the Goldman equation for a system with a single permeable ion could be expected if the outer membrane were permeable to ions other than Na^+ as suggested by the fact that E_o is smaller than likely values of the electrochemical potential of sodium (Rick, Dörge, Von Arnim & Thurau, 1978; Nagel, Garcia-Diaz & Armstrong, 1981). However, application of the Goldman current equation may be inadequate if the outer membrane permeability is intrinsically voltage dependent. Such voltage dependence of the outer membrane sodium channel has previously been hypothetized (Grinstein et al., 1978; Goudeau et al., 1979) and is confirmed by recent analysis involving microelectrode techniques (Nagel & Essig, *Pfluegers Arch., submitted*). Lindemann and Van Driessche (1977) have pointed out that the sodium channel fluctuates between an open and a closed state. It is then possible that the outer membrane depolarization might shift the equilibrium open⇆closed state towards the closed state.

Inner Membrane Current-Voltage Curve Obviously the graphical determination of R_{i1} is relatively imprecise and this would make the numerical values obtained somewhat unreliable. Nevertheless, the inner membrane has a nonlinear behavior which, although less pronounced than the outer one, shows a sharper transition in the $I_{Na}-V_i$ than in the $I_{Na}-V_o$ curve. This nonlinearity of the $I_{Na}-V_i$ curve is at variance with the results of Helman and Fisher (1977) for *Rana pipiens*, who obtained a linear relation between V_i and I_{Na}. The discrepancy may come from the fact that the contribution of an external applied transepithelial potential to V_o and V_i depends on the R_o/R_i ratio, and this ratio is higher in the experiments of Helman and Fisher (1977), than in ours. As a direct consequence of the present inner rectification, the graphically determined value of E_i is, in absolute terms, smaller than it would be if R_i were constant (100.8 ± 2.5 mV against 108.7 ± 2.3 mV). The rectification at the inner border could be the well-known anomalous rectification described in frog muscle membrane.

Effects of La^{3+}

La^{3+} added on the mucosal side raises the I^{sc} and depolarizes the epithelial cells. This may be due to

modifications of electromotive and/or conductive components at the outer and inner borders of the epithelial cells. The effect of La^{3+} on conductance is obvious: it reduces R_{o1} and R_{o2}, but not to the same extent (Fig. 5*b* and Table 1), since R_{o1} and R_{o2}, respectively, drop to 28 and 52% of the control values and the rectification ratio R_{o1}/R_{o2} falls from 3.30 on control skins to 1.80 after La^{3+}. On experimental skins mean value of R_{o1} (but not R_{o2}) are significantly different (at $p=0.05$) from the corresponding control values. However, the mean difference between experimental and control values of paired skins is significantly different from zero (at $0.01<p<0.001$ for R_{o1} and $0.02<p<0.01$ for R_{o2}) as ascertained by the Student *t*-test.

We started on the basis of the hypothesis that surface potential affects the conductance of the outer border sodium channel (Grinstein et al., 1978; Goudeau et al., 1979). If such a negative surface potential (Naharashi, 1966; Ito, Kuriyama & Tashiro, 1970; D'Arrigo, 1973) is reduced by La^{3+} on the outer side of the membrane, this leads to an increase in the intramembrane inward electrical field. In view of the above evidence of the voltage dependency of the apical border sodium conductance (with an increased conductance when the cell hyperpolarizes) such a La^{3+}-induced rise in the electrical field could produce the observed sodium conductance increase.

La^{3+} increases E_o in a nonsignificant fashion (Table 1), but as in the case of R_o values, the mean difference between experimental and control E_o values of paired skins are indeed highly different from zero ($p<0.001$). The fact that La^{3+} increases E_o to more positive values (Table 1), can be considered merely as the result of an increase in sodium conductance relative to other ions. From Eq. (8) it is evident that such a change of E_o in connection with an increase in R_i/R_o should affect the value of E_1'. Our results show that E_1' indeed decreases. Accordingly, it is not necessary to assume that La^{3+} affects the electromotive force of the inner border, a conclusion which is in agreement with our observation that $E'_{1\,amil}$ remained unchanged after La^{3+}. Similarly the resistance of the inner border is only slightly decreased (in the R_{i2} range) or not modified (in the R_{i1} range or calculated from $\Delta V_o^{sc}/I_{Na}^{sc}$). Thus as postulated previously (Goudeau et al., 1979) the early affect of La^{3+} is indeed restricted to the apical barrier.

Long-Term Effects of La^{3+}

Table 2 shows that 1 hr after La^{3+} the outer membrane conductance decreases secondarily; this phenomenon especially affects R_{o2} which returns to its initial control value, and to a lesser extent R_{o1}. Compared with these changes in the outer membrane conductance, the inner membrane conductance is relatively unaffected. As assumed previously (Goudeau et al., 1979), the inhibitory effect of La^{3+} on I^{sc} may be related to penetration of this trivalent ion into the sodium channel, driven by the electrical field. This would explain that the inhibitory secondary effect of La^{3+} is only clearly visible on normally polarized skins (Wietzerbin et al., 1977).

References

Biber, T.U.L., Sanders, M.L. 1973. Influence of transepithelial potential difference on the sodium uptake at the outer surface of the isolated frog skin. *J. Gen. Physiol.* **61**:529–551

Crabbé, J. 1968. A hypothesis concerning the mode of action of amiloride and triamterene. *Arch. Int. Pharmacodyn. Ther.* **173**:474–477

Cuthbert, A.W., Shum, W.K. 1976. Characteristics of the entry process for sodium in transporting epithelia as revealed with amiloride. *J. Physiol. (London)* **255**:587–604

D'Arrigo, J.S. 1973. Possible screening of surface charges on crafish axons by polyvalent metal ions. *J. Gen. Physiol.* **231**:117–128

De Sousa, R.C. 1975. Mécanismes de transport de l'eau et du sodium par les cellules des épithelia d'Amphibiens et du tubule rénal isolé. *J. Physiol. (Paris)* **71**:5A–71A

Dörge, A., Nagel, W. 1970. Effect of amiloride on sodium transport in frog skin. II. Sodium transport pool and unidirectional fluxes. *Pfluegers Arch,* **321**:91–101

Finkelstein, A., Mauro, A. 1963. Equivalent circuit as related to ionic systems. *Biophys. J.* **3**:215–237

Fuchs, W., Hviid Larsen, E., Lindemann, B. 1977. Current-voltage curve of sodium channels and concentration dependence of sodium permeability in frog skin. *J. Physiol. (London)* **267**:137–166

Goldman, D.E. 1943. Potential, impedance and rectification in membrane. *J. Gen. Physiol.* **27**:37–60

Goudeau, H., Wietzerbin, J., Gary-Bobo, C.M. 1979. Effects of mucosal lanthanum on electrical parameters of isolated frog skin mechanisms of action. *Pfluegers Arch,* **379**:71–80

Grinstein, S., Candia, O., Erlij, D. 1978. Nonhormonal mechanisms for the regulation of transepithelial sodium transport: The roles of surface potential and cell calcium. *J. Membrane Biol.* **Special Issue**:261–280

Helman, S.I. 1979. Electrochemical potentials in frog skin: Inferences for electrical and mechanistic models. *Fed. Proc.* **38**:2743–2750

Helman, S.I., Fisher, R.S. 1977. Microelectrode studies of the active Na transport pathway of frog skin. *J. Gen. Physiol.* **69**:571–604

Helman, S.I., Miller, D.A. 1971. *In vitro* techniques for avoiding edge damage in studies of frog skin. *Science* **176**:146–148

Ito, Y., Kuriyama, H., Tashiro, N. 1970. Effects of divalent cations on spike generation in the longitudinal somatic muscle of the earth worm. *J. Exp. Biol.* **52**:79–94

Koefoed-Johnsen, V., Ussing, H.H. 1958. The nature of the frog skin potential. *Acta Physiol. Scand.* **42**:298–308

Lindemann, B., Van Driessche, W. 1977. Sodium specific membrane channels of frog skin are pores: Current fluctuations reveal high turnover. *Science* **195**:292–294

Macchia, D., Helman, S.I. 1979. Transepithelial current voltage

relationships of toad urinary bladder and colon. Estimates of E_{Na} and shunt resistance. *Biophys. J.* **27**:371–392

Macknight, A.C.D., Dibona, D.R., Leaf, A. 1980. Sodium transport across toad urinary bladder: A model "tight" epithelium. *Physiol. Rev.* **60**:615–715

Martinez-Palomo, A., Erlij, D., Bracho, H. 1971. Localization of permeability barriers in the frog skin epithelium. *J. Cell Biol.* **50**:277–287

Nagel, W. 1976. The intracellular electrical potential profile of the frog skin epithelium. *Pfluegers Arch.* **365**:135–143

Nagel, W. 1977. The dependence of the electrical potentials across the membranes of the frog skin upon the concentration of sodium in the mucosal solution. *J. Physiol. (London)* **269**:777–796

Nagel, W. 1978. Effects of antidiuretic hormone upon electrical potential and resistance of apical and basolateral membranes of frog skin. *J. Membrane Biol.* **42**:99–122

Nagel, W. 1980. Rheogenic sodium transport in a tight epithelium, the amphibian skin. *J. Physiol. (London)* **302**:281–295

Nagel, W., Garcia-Diaz, J.F., Armstrong, W. 1981. Intracellular ionic activities in frog skin. *J. Membrane Biol.* **61**:127–134

Naharashi, T. 1966. Dependence of excitability of the cockroach giant axons on external divalent cations. *Comp. Biochem. Physiol.* **19**:759–774

Rick, R., Dörge, A., Von Arnim, E., Thurau, K. 1978. Electron microprobe analysis of frog skin epithelium: Evidence of a syncytial sodium transport compartment. *J. Membrane Biol.* **39**:313–331

Schultz, S.G. 1979. Application of equivalent electrical circuit models to the study of sodium transport across epithelial tissues. *Fed. Proc.* **38**:2024–2030

Schultz, S.G., Frizzell, R.A., Nellans, H.N. 1977. An equivalent electrical circuit model for "sodium-transporting" epithelia in the steady-state. *J. Theor. Biol.* **65**:215–229

Ussing, H.-H., Zerahn, I. 1951. Active transport of sodium as the source of electric current in the short-circuited isolated frog skin. *Acta Physiol. Scand.* **23**:110–117

Wietzerbin, J., Goudeau, H., Gary-Bobo, C.M. 1977. Influence of membrane polarization and hormonal stimulation on the action of lanthanum on frog skin sodium permeability. *Pfluegers Arch.* **370**:145–153

Received 4 May 1981; revised 15 September 1981